Bimetallic Synergism in Alkyne Silylformylation Catalyzed by a Cobalt−Rhodium Mixed-Metal Cluster

Naohiko Yoshikai,[†] Masahiro Yamanaka,[†] Iwao Ojima,[‡] Keiji Morokuma,[§] and Eiichi Nakamura*[,†]

Department of Chemistry, The University of Tokyo, Bunkyo-ku, Tokyo 113-0033, Japan, Department of Chemistry, State University of New York at Stony Brook, Stony Brook, New York 11794-3400, and Department of Chemistry, Emory University, Atlanta, Georgia 30322

Received May 31, 2006

A cobalt−rhodium mixed-metal carbonyl complex $Co_2Rh_2(CO)_{12}$ effects efficient catalytic silylformylation of an alkyne that adds silyl and formyl groups across the C−C triple bond. A bimetallic synergism in this reaction was elucidated with density functional calculations. The catalytic cycle consists of oxidative addition of hydrosilane, alkyne insertion, CO insertion, and reductive elimination. While major bond-forming events take place only at the rhodium center, the cobalt also plays an important role; it fixes the metal cluster on the organic substrate, keeps the hydride ligand temporarily on the metal center, and suppresses hydrosilylation, which would otherwise be preferred over the silylformylation. The Rh and Co atoms exchange electrons with each other, giving rise to a unique bimetallic reaction pathway that is related to but different from the conventional pathways of hydroformylation and hydrosilylation.

Multimetallic homogeneous catalysis has received much attention from chemists working on catalysis,[1] since it offers possibilities of unusual reactivities and/or selectivities that are not attainable by monometallic systems. Multimetallic catalytic systems include various types of metal−metal combinations, that is, transition metal (TM)−main group metal (MM), MM−MM, MM−rare earth (RE) metal, and TM−TM. Metals may act as independent species or may be included in a single reactive species. Of great interest from an organometallic perspective are the catalytic systems involving metal−metal bonds. Such systems involve simultaneous oxidation/reduction of multiple metals in one elementary step and may serve as a mechanistic bridge between homogeneous and heterogeneous catalysis. The mechanism of multimetallic synergism therefore has been among the central interests of ours as well as others.[2−5] We previously reported on the mechanisms of several synthetically important organic transformations of homobimetallic and homotrimetallic clusters with the aid of density functional calculations.[2,3] One typical example is the Pauson−Khand (PK) reaction, a $Co_2(CO)_8$-catalyzed synthesis of cyclopentenone from alkyne, alkene, and carbon monoxide.[6,7] The cobalt cluster forms a butterfly-like complex with an alkyne, and the dicobalt framework is kept during the catalytic cycle. Our previous theoretical study revealed the cooperation of the two cobalt centers in this reaction:[3a,8] C−C bond-forming events take place on one of the two cobalt atoms, and the other acts as an anchor to the first, exerting electronic influences on the first through the metal−metal bond.

Heteromultimetallic catalysis is even more interesting than homometallic catalysis, since it can offer much more diverse reactivities and mechanistic complexities. Although examples of useful reactions initiated by addition of a multimetallic catalyst exist,[9] evidence for maintenance of the multimetallic integrity and/or the role of the metal−metal bond in the catalyst has seldom been observed. The example of bimetallic catalyst reported by Ojima et al. in 1991 is an exceptional case,[10] because of the presence of several lines of indirect evidence that it involves a multimetallic catalysis. They found that the cobalt−

* To whom correspondence should be addressed. E-mail: nakamura@chem.s.u-tokyo.ac.jp.

[†] The University of Tokyo.

[‡] State University of New York at Stony Brook.

[§] Emory University.

(1) (a) *Catalysis by Di- and Polynuclear Metal Cluster Complexes*; Adams, R. D., Cotton, A., Eds.; Wiley-VCH: New York, 1998. (b) Chetcuti, M. J. In *Comprehensive Organometallic Chemistry II*; Adams, R. D., Ed.; Pergamon Press: Oxford, U.K., 1995; Vol. 10. (c) *Multimetallic Catalysts in Organic Synthesis*; Shibasaki, M., Yamamoto, Y., Eds.; Wiley-VCH: Weinheim, 2004.

(2) (a) Khoroshun, D. V.; Inagaki, A.; Suzuki, H.; Vyboishchikov, S. F.; Musaev, D. G.; Morokuma, K. *J. Am. Chem. Soc.* **2003**, *125*, 9910−9911. (b) Musaev, D. G.; Nowroozi-Isfahani, T.; Morokuma, K.; Rosenburg, E. *Organometallics* **2005**, *24*, 5973−5982. (c) Musaev, D. G.; Nowroozi-Isfahani, T.; Morokuma, K.; Abedin, J.; Rosenburg, E.; Hardcastle, K. I. *Organometallics* **2006**, *25*, 203−213.

(3) (a) Yamanaka, M.; Nakamura, E. *J. Am. Chem. Soc.* **2001**, *123*, 1703−1708. (b) Nakamura, E.; Yoshikai, N.; Yamanaka, M. *J. Am. Chem. Soc.* **2002**, *124*, 7181−7192. (c) Ammal, S. C.; Yoshikai, N.; Inada, Y.; Nishibayashi, Y.; Nakamura, E. *J. Am. Chem. Soc.* **2005**, *127*, 9428−9438.

(4) (a) Li, C.; Widjaja, E.; Garland, M. *J. Am. Chem. Soc.* **2003**, *125*, 5540−5548. (b) Li, C.; Widjaja, E.; Garland, M. *Organometallics* **2004**, *23*, 4131−4138.

(5) Fukuoka, A.; Fukagawa, S.; Hirano, M.; Koga, N.; Komiya, S. *Organometallics* **2001**, *20*, 2065−2075.

(6) (a) Khand, I. U.; Knox, G. R.; Pauson, P. L.; Watts, W. E. *J. Chem. Soc., Chem. Commun.* **1971**, 36. (b) Khand, I. U.; Knox, G. R.; Pauson, P. L.; Watts, W. E. *J. Chem. Soc., Perkin Trans. 1* **1973**, 975−977. (c) Khand, I. U.; Knox, G. R.; Pauson, P. L.; Watts, W. E.; Foreman, M. I. *J. Chem. Soc., Perkin Trans. 1* **1973**, 977−981.

(7) (a) Geis, O.; Schmalz, H.-G. *Angew. Chem., Int. Ed.* **1998**, *37*, 911−914. (b) Chung, Y. K. *Coord. Chem. Rev.* **1999**, *188*, 297−341. (c) Fletcher, A. J.; Christie, S. D. R. *J. Chem. Soc., Perkin Trans. 1* **2000**, 1657−1668. (d) Brummond, K. M.; Kent, J. L. *Tetrahedron* **2000**, *56*, 3263−3283. (e) Sugihara, T.; Yamaguchi, M.; Nishizawa, M. *Chem. Eur. J.* **2001**, *7*, 1589−1595.

(8) (a) Robert, F.; Milet, A.; Gimbert, Y.; Konya, D.; Greene, A. E. *J. Am. Chem. Soc.* **2001**, *123*, 5396−5400. (b) De Bruin, T. J. M.; Milet, A.; Robert, F.; Gimbert, Y.; Greene, A. E. *J. Am. Chem. Soc.* **2001**, *123*, 7184−7185.

(9) Ishii, T.; Hidai, M. In *Multimetallic Catalysts in Organic Synthesis*; Shibasaki, M., Yamamoto, Y., Eds.; Wiley-VCH: Weinheim, 2004; pp 201−223, and references therein.

(10) (a) Ojima, I.; Ingallina, P.; Donovan, R. J.; Clos, N. *Organometallics* **1991**, *10*, 38−41. (b) Ojima, I.; Li, Z.; Donovan, R. J.; Ingallina, P. *Inorg. Chim. Acta* **1998**, *270*, 279−284.

10.1021/om060478x CCC: $33.50
Publication on Web 07/06/2006

rhodium mixed-metal cluster $Co_2Rh_2(CO)_{12}$ (**I**) is an effective catalyst for a silylformylation reaction of an alkyne at room temperature (eq 1) and that the reactive species most likely involves one Rh and one Co atom (vide infra). The same synthetic transformation was independently discovered by Matsuda,[11] who instead used a $Rh_4(CO)_{12}/NEt_3$ catalyst at much higher temperature. Several metal complexes including carbonyl clusters such as **I**, $Rh_4(CO)_{12}$,[14,15] and $(CO)_4CoRh(CN\mathit{t}Bu)_4$, and rhodium complexes such as $Rh(acac)(CO)_2$,[12] $Rh_2(pfb)_4$ (pfb = perfluorobutylate),[13] and $[Rh(COD)]^+BPh_4^-$,[14] have been found to catalyze the silylformylation reaction. Carbonyl clusters such as $Co_2(CO)_8$ and $Ru_3(CO)_{12}$ showed no catalytic activity.[15]

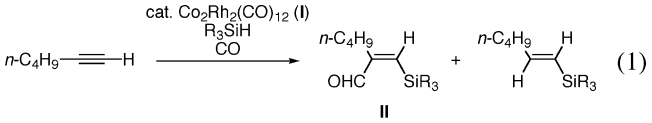

(1)

The mixed-metal cluster **I** has several advantages over other catalysts. First, it promotes the silylformylation reaction under milder conditions (i.e., ambient temperature and CO pressure) than other Rh catalytic systems (heat (40−100 °C) and/or positive CO pressure (10−50 atm)).[14,15,17,18] It is notable that the mononuclear Wilkinson complex $RhCl(PPh_3)_3$, which catalyzes the hydrosilylation reaction, does not catalyze the silylformylation reaction at all. The second advantage is the high selectivity of the reaction. While the homonuclear cluster $Rh_4(CO)_{12}$ is as reactive as **I**, the latter shows high selectivity for silylformylation/hydrosilylation as well as stereoselectivity of the C−C double bond (*cis*-addition).[14,15] While Matsuda et al. proposed monometallic active species in their $Rh_4(CO)_{12}/NEt_3$-catalyzed silylformylation reaction,[15b] Ojima suggested on the basis of experimental data (vide infra) that a Co−Rh bimetallic species is essential for the unique reactivity/selectivity of his own mixed-metal-catalyzed silylformylation.[14] The mechanism of the action of the Co and Rh atoms in the Ojima reaction is the subject of the present study.

Regardless of the nuclearity of the catalytically active species, Rh has been accepted as the critically important metal for the silylformylation. On the basis of the kinship between the Rh-catalyzed hydrosilylation and the hydroformylation reactions, there have been suggested two mechanisms for the silylformylation (Scheme 1, a and b).[15b] Both consist of the same elementary steps but in a different sequence: oxidative addition of a hydrosilane to the Rh atom (step i), alkyne insertion into the Rh−Si bond (ii), carbonyl insertion into the Rh−vinyl bond (iii), reductive elimination of an aldehyde (iv). In terms of the Rh oxidation state, these two mechanisms are related to those of the Rh-catalyzed hydrosilylation and the hydroformylation, respectively.[15,16] In the former mechanism, alkyne insertion (ii) and CO insertion (iii) take place at the Rh^{III} oxidation state, but, in the latter, at the Rh^{I} state.

How then can the Co atom take part in such catalytic cycles and enhance the efficiency of the silylformylation reaction? Several experimental results suggest involvement of bimetallic catalytic species in the $Co_2Rh_2(CO)_{12}$-catalyzed silylformylation.[14b] First, the reaction of the tetranuclear cluster **I** with a hydrosilane under CO atmosphere gives Co−Rh bimetallic complexes $(CO)_3Co-Rh(CO)_n(SiR_3)_2$ **IIIa** (n = 2) and **IIIb** (n = 3) (Scheme 2). A stoichiometric reaction of **IIIa** and **IIIb** with 1-hexyne and carbon monoxide affords the *Z*-silylformylation product **II** along with 5% of its *E*-isomer. Second, **I** reacts with 1-hexyne under carbon monoxide to give a Co−Rh bimetallic butterfly-type complex, **IV** (Scheme 3). The reaction of **IV** with the hydrosilane under carbon monoxide affords exclusively the *Z*-silylformylation product, as in the actual catalytic reaction. Thus, the bimetallic complex **IV** is likely to be a catalytic species in the silylformylation reaction.

With the above background, we explored the reaction mechanism of the Co−Rh cluster-catalyzed silylformylation reaction by density functional calculations. On the basis of the computational results, we propose a catalytic cycle where both of the metal atoms are deeply involved in each elementary step. While most of the organic transformations take place at the Rh center, the Co atom also plays important roles: It assists binding of the acetylene and the hydride to the coordination sphere of the Rh atom and also acts as an electron reservoir during the catalytic cycle. The second metal is therefore critical both for efficient silylformylation and for the high stereoselectivity of the reaction.

Computational Methods

All calculations were performed with Gaussian 98 and Gaussian 03 program packages.[17] Density functional theory (DFT) was employed using the B3LYP hybrid functional.[18] Structures were optimized with a basis set (denoted as 631LAN) consisting of the LANL2DZ basis set including a double-ζ valence basis set with the Hay and Wadt effective core potential (ECP)[19] for Co and Rh,

(11) (a) Matsuda, I.; Ogiso, A.; Sato, S.; Izumi, Y. *J. Am. Chem. Soc.* **1989**, *111*, 2332−2333. (b) Matsuda, I.; Fukuta, Y.; Tsuchihashi, T.; Nagashima, H.; Itoh, K. *Organometallics* **1997**, *16*, 4327−4345.

(12) Ojima, I.; Vidal, E.; Tzamarioudaki, M.; Matsuda, I. *J. Am. Chem. Soc.* **1995**, *117*, 6797−6798.

(13) Doyle, M. P.; Shanklin, M. S. *Organometallics* **1994**, *13*, 1081−1088.

(14) Zhou, J.-Q.; Alper, H. *Organometallics* **1994**, *13*, 1586−1591.

(15) (a) Ojima, I. In *The Chemistry of Organic Silicon Compounds*; Patai, S., Rappoport, Z., Eds.; John Wiley & Sons: New York, 1989; p 1415. (b) Sakaki, S.; Sumimoto, M.; Fukuhara, M.; Sugimoto, M.; Fujimoto, H.; Matsuzaki, S. *Organometallics* **2002**, *21*, 3788−3802, and references therein.

(16) (a) Koga, N.; Morokuma, K. *Chem. Rev.* **1991**, *91*, 823−842. (b) Torrent, M.; Solà, M.; Frenking, G. *Chem. Rev.* **2000**, *100*, 439−493, and references therein.

(17) Frisch, M. J.; Trucks, G. W.; Schlegel, H. B.; Scuseria, G. E.; Robb, M. A.; Cheeseman, J. R.; Zakrzewski, V. G.; Montogomery, J. A., Jr.; Stratmann, R. E.; Burant, J. C.; Dapprich, S.; Millam, J. M.; Daniels, A. D.; Kudin, K. N.; Strain, M. C.; Farkas, O.; Tomasi, J.; Barone, V.; Cossi, M.; Cammi, R.; Mennucci, B.; Pomelli, C.; Adamo, C.; Clifford, S.; Ochterski, J.; Petersson, G. A.; Ayala, P. Y.; Cui, Q.; Morokuma, K.; Malick, D. K.; Rabuck, A. D.; Raghavachari, K.; Foresman, J. B.; Cioslowski, J.; Ortiz, J. V.; Baboul, A. G.; Stefanov, B. B.; Liu, G.; Liashenko, A.; Piskorz, P.; Komaromi, I.; Gomperts, R.; Martin, R. L.; Fox, D. J.; Keith, T.; Al-Laham, M. A.; Peng, C. Y.; Nanayakkara, A.; Challacombe, M.; Gill, P. M. W.; Johnson, B.; Chen, W.; Wong, M. W.; Andres, J. L.; Gonzalez, C.; Head-Gordon, M.; Pople, J. A. *Gaussian 98*, revision A.9; Gaussian. Inc.: Pittsburgh, PA, 1998. Frisch, M. J.; Trucks, G. W.; Schlegel, H. B.; Scuseria, G. E.; Robb, M. A.; Cheeseman, J. R.; Montgomery, J. A., Jr.; Vreven, T.; Kudin, K. N.; Burant, J. C.; Millam, J. M.; Iyengar, S. S.; Tomasi, J.; Barone, V.; Mennucci, B.; Cossi, M.; Scalmani, G.; Rega, N.; Petersson, G. A.; Nakatsuji, H.; Hada, M.; Ehara, M.; Toyota, K.; Fukuda, R.; Hasegawa, J.; Ishida, M.; Nakajima, T.; Honda, Y.; Kitao, O.; Nakai, H.; Klene, M.; Li, X.; Knox, J. E.; Hratchian, H. P.; Cross, J. B.; Adamo, C.; Jaramillo, J.; Gomperts, R.; Stratmann, R. E.; Yazyev, O.; Austin, A. J.; Cammi, R.; Pomelli, C.; Ochterski, J. W.; Ayala, P. Y.; Morokuma, K.; Voth, G. A.; Salvador, P.; Dannenberg, J. J.; Zakrzewski, V. G.; Dapprich, S.; Daniels, A. D.; Strain, M. C.; Farkas, O.; Malick, D. K.; Rabuck, A. D.; Raghavachari, K.; Foresman, J. B.; Ortiz, J. V.; Cui, Q.; Baboul, A. G.; Clifford, S.; Cioslowski, J.; Stefanov, B. B.; Liu, G.; Liashenko, A.; Piskorz, P.; Komaromi, I.; Martin, R. L.; Fox, D. J.; Keith, T.; Al-Laham, M. A.; Peng, C. Y.; Nanayakkara, A.; Challacombe, M.; Gill, P. M. W.; Johnson, B.; Chen, W.; Wong, M. W.; Gonzalez, C.; Pople, J. A. *Gaussian 03*, Revision C.02; Gaussian, Inc.: Wallingford, CT, 2004.

(18) (a) Becke, A. D. *J. Chem. Phys.* **1993**, *98*, 5648−5652. (b) Lee, C.; Yang, W.; Parr, R. G.; *Phys. Rev. B* **1988**, *37*, 785−789.

(19) Wadt, W. R.; Hay, P. J. *J. Chem. Phys.* **1985**, *82*, 299−310.

Scheme 1. Catalytic Cycles Proposed for Rh-Catalyzed Silylformylation Reaction

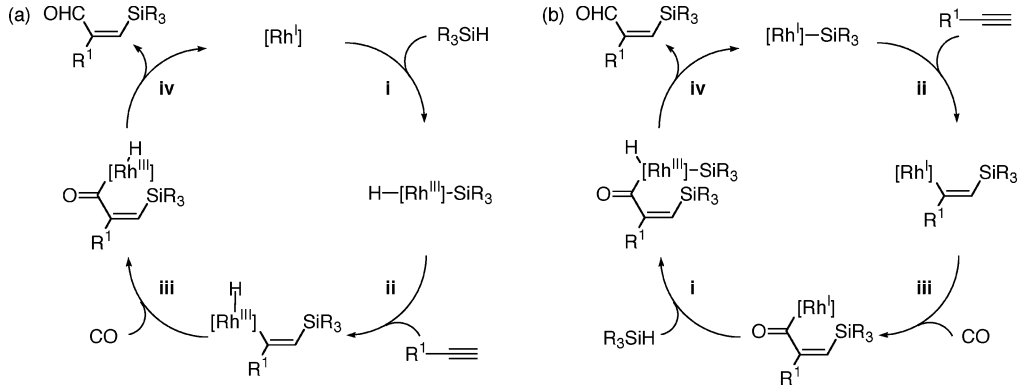

Scheme 2

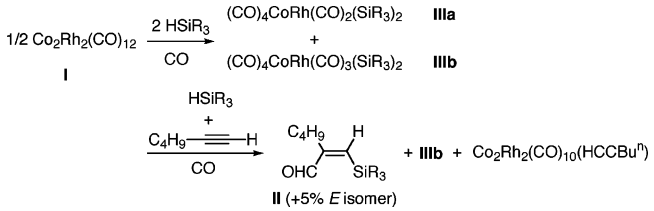

Scheme 3

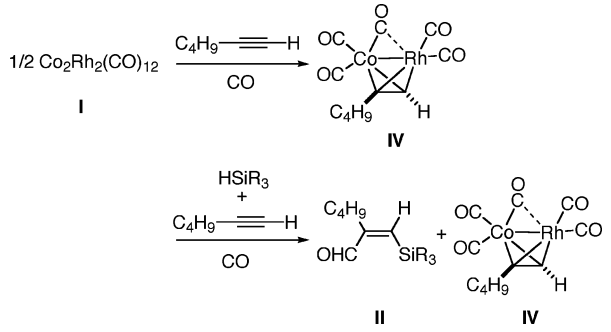

and the 6-31G(d) basis set[20] for C, H, O, and Si. The method and the basis sets used here have been known to give reliable results for the structures and reactivities of Co−Co or Rh−Rh dinuclear complexes.[3ab] All structures were optimized without symmetry assumption unless otherwise noted. Stationary points on the major reaction pathway were adequately characterized by normal coordinate analysis.[21] The intrinsic reaction coordinate (IRC) analysis[22] was carried out for the major reaction pathway to confirm that all stationary points are smoothly connected with each other. While essentially all structural and conformational possibilities of ligand coordination, those in the final hydride transfer stage in particular, have been considered, only the most facile pathway along the IRC is described below. Higher-level single-point energy calculations were performed for the B3LYP/631LAN-optimized structures using larger basis sets denoted as 6311SDD, consisting of the Stuttgart ECP[23] for Co and Rh and the 6-311G(d,p) for the rest, and the potential energies (*E*) that are shown in the energy diagrams and discussed in the text are based on these single-point calculations (B3LYP/6311SDD//B3LYP/631LAN). *E*, *E* + ZPE (zero-point energy), *H* (enthalpy), and *G* (Gibbs free energy) calculated at the B3LYP/631LAN level are given in the Supporting Information. Natural population analysis was performed at the same level as the one used for geometry optimization.[24]

Results and Discussion

On the basis of experimental results described above (Scheme 3), we employed a Co−Rh complex of $CoRh(C_2H_2)(CO)_5$ stoichiometry as an initial complex for the present study. The silylformylation pathways were explored by sequential introduction of Me_3SiH and CO to this complex. Scheme 4 and Figure 1 show the summary of the reaction pathway and energetics of the Co−Rh-catalyzed silylformylation proposed in this article. The catalytic cycle starts from the butterfly-type complex **1** (or **2**) and involves the following steps: oxidative addition of Me_3SiH (**1** → **3** or **1** → **4**), isomerization of the oxidative addition product to a hydride-bridged complex **5** (**3** → **5** or **4** → **5**), acetylene insertion into the Rh−Si bond (**5** → **6**), CO insertion into the Rh−vinyl bond (**7** → **8**), hydride migration from Co to Rh (**8** → **9**), and reductive elimination (**9** → **10**). Exchange of the product with another acetylene molecule completes the catalytic cycle. The outline of this mechanism is similar to the one originally proposed by Ojima et al. in 1991,[14a] but not to the one suggested in 1998,[14b] which involves a bis-alkyne complex as a key intermediate.[25] Details of each step will be described hereafter.

Starting Complex. First, we explored the structural possibilities of the butterfly complex $CoRh(CO)_5(C_2H_2)$. Among several optimized structures, complexes **1** and **2** were found to be more stable than others by as much as >10 kcal/mol at the B3LYP/631LAN level (Figure 2, see Supporting Information for other structures). While the Co and Rh atoms are directly bonded in **1**, they are bridged by a carbonyl ligand in **2**. The energy difference of **1** and **2** is calculated to be only 1.0 kcal/mol, and interconversion between them takes place readily through a transition state $\mathbf{TS_{1-2}}$ ($\Delta E^{\ddagger} = 1.9$ kcal/mol from **1**). Although a CO semibridging structure **IV** was indicated for the isolated complex with 1-hexyne on the basis of the IR absorption of 1935 cm^{-1} (Scheme 3),[14] such a structure could not be located as an equilibrium structure but existed as $\mathbf{TS_{1-2}}$.[26] In light of the extremely flat potential surface along the IRC between **1**

(20) Hehre, W. J.; Radom, L.; Schleyer, P. v R.; Pople, J. A. *Ab Initio Molecular Orbital Theory*; John Wiley & Sons: New York, 1986, and references therein.

(21) Other structures were characterized by the eigenvalues of the Hessian matrixes (no negative eigenvalue for an equilibrium structure and one negative eigenvalue for a transition structure).

(22) (a) Fukui, K. *Acc. Chem. Res.* **1981**, *14*, 363−368. (b) Gonzalez, C.; Schlegel, H. B. *J. Chem. Phys.* **1989**, *90*, 2154−2161. Gonzalez, C.; Schlegel, H. B. *J. Phys. Chem.* **1990**, *94*, 5523−5527.

(23) Dolg, M.; Wedig, U.; Stoll, H.; Preuss, H. *J. Chem. Phys.* **1987**, *86*, 866−872.

(24) Reed, A. E.; Weinstock, R. B.; Weinhold, F. *J. Chem. Phys.* **1985**, *83*, 735−746. Reed, A. E.; Curtiss, L. A.; Weinhold, F. *Chem. Rev.* **1988**, *88*, 899−926. Glendening, E. D.; Reed, A. E.; Carpenter, J. E.; Weinhold, F. *NBO Version 3.1* in the Gaussian 98 package; University of Wisconsin: Madison, WI, 1990.

(25) This possibility was discarded in the early stage of the study because of unreasonably high energy of a bis-alkyne complex.

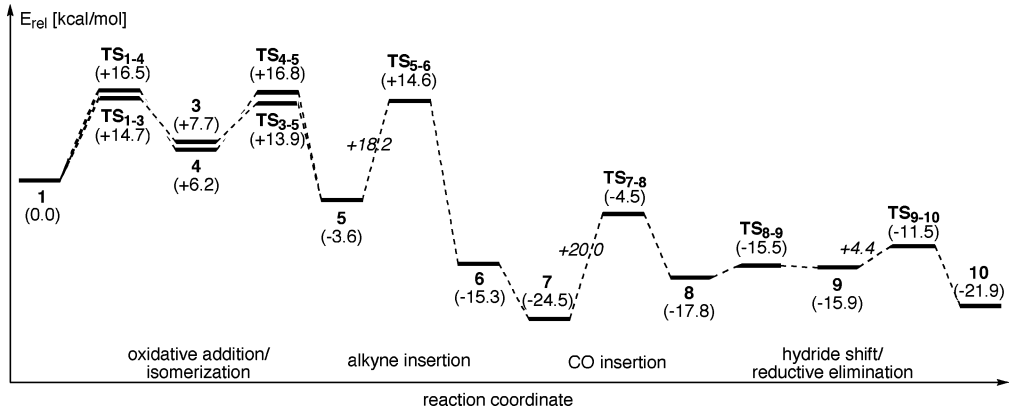

Figure 1. Potential energy diagram (in kcal/mol) of the silylformylation reaction calculated at the B3LYP/6311SDD//B3LYP/631LAN level.

Scheme 4. Bimetallic Pathway of the Silylformylation Reaction

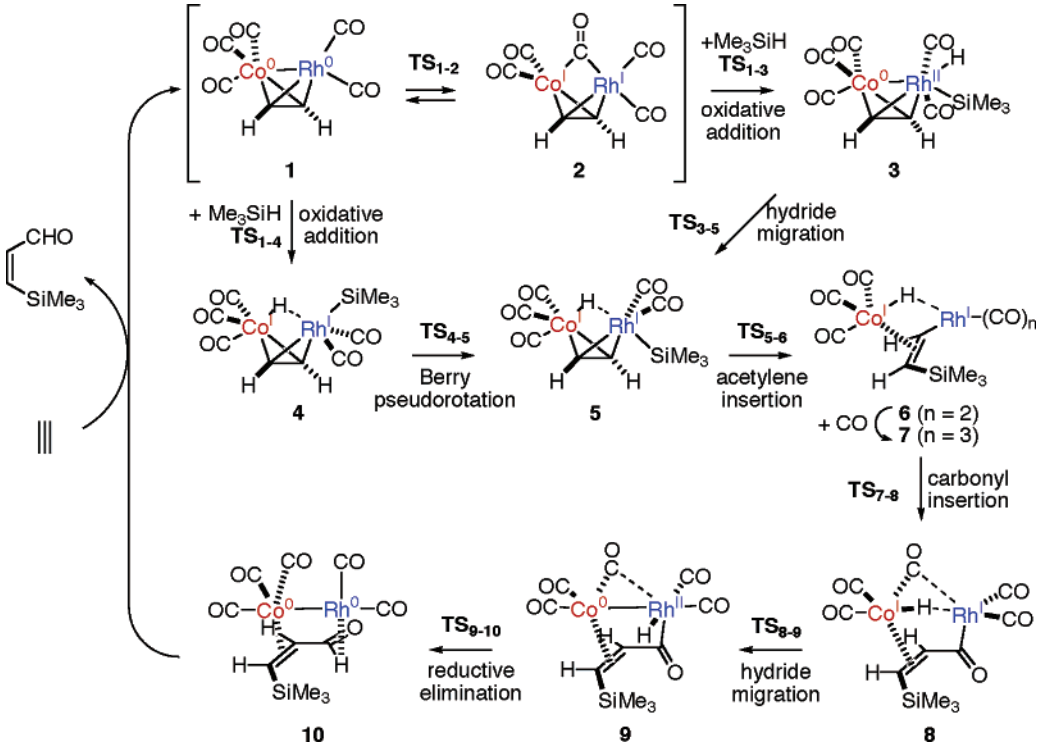

(no CO bridge), **TS**$_{1-2}$, and **2** (CO fully bridged) (maximum activation energy of 1.9 kcal/mol), we consider that this inconsistency is rather insignificant and is likely due to the deficiency of the theoretical model or due to the difference of the chemical models including the difference of the gas versus solution phases.

The structure of the butterfly moiety of the complex **1** (and **2**) gives us information on the interaction between the two metals and the acetylene ligand (Figure 2). Acetylene is positioned well so that its two orthogonal π orbitals interact with Co and Rh, respectively. Significant bending of the acetylene ligand in **1** (C^2-C^1-H bond angle = 145.0°, not indicated in Figure 2) indicates strong π-back-donation. The much larger $Co-C^2-C^1-H$ dihedral angle (157.5°) than the $Rh-C^1-C^2-H$ angle (125.0°) in **1** suggests that the metal-to-acetylene back-donation occurs mainly from the Co atom. Therefore, if acetylene is considered to have formed a metallacycle, **1** can be regarded mainly as a cobalta(II)cyclopropene. Thus, it is reasonable to consider that the oxidative addition of a hydrosilane takes place on the Rh atom.

Oxidative Addition of Hydrosilane. Since a number of possible approaches of a hydrosilane molecule (Me_3SiH) to the Co−Rh complex complicated our study,[27] we first examined the product structures, that is, various possible isomers of the Me_3SiH oxidative addition product. As a result, among optimized structures, the hydride-bridged complex **5** was found to be more stable than the other isomers by as much as ca. 10 kcal/mol at the B3LYP/631LAN level (Scheme 5, see also Supporting Information). In addition, the study on the next step (i.e., acetylene insertion into the Rh−Si bond) revealed that **5** is a key intermediate connected to a low-energy TS (vide infra, see Supporting Information). With these results in hand, we carried out further calculations to find two pathways (**1** → **3** → **5** (path a) and **1** → **4** → **5** (path b)) connecting the initial

(26) We also carried out geometry optimization of a complex with 1-hexyne and also obtained two local minima essentially the same as **1** and **2** of much the same energy (energy difference < 1.0 kcal/mol) instead of a semibridged stable structure.

(27) Sakaki, S.; Ujino, Y.; Sugimoto, M. *Bull. Chem. Soc. Jpn.* **1996**, *69*, 3047−3057.

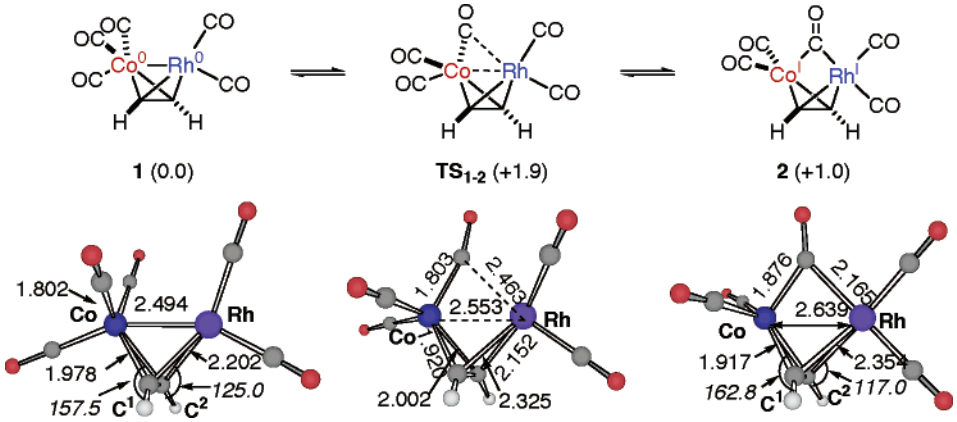

Figure 2. Structures of the initial complexes **1** and **2** and the TS of interconversion between them ($\mathbf{TS}_{1-2}$) optimized at the B3LYP/631LAN level. Numbers in parentheses refer to potential energies (kcal/mol, at the B3LYP/6311SDD//B3LYP/631LAN level) relative to **1**. Numbers shown in the 3-D structures indicate distances (Å) and dihedral angles (italicized, deg).

Scheme 5. Two Pathways for Oxidative Addition of Me_3SiH to 1 and Subsequent Isomerization to 5[a]

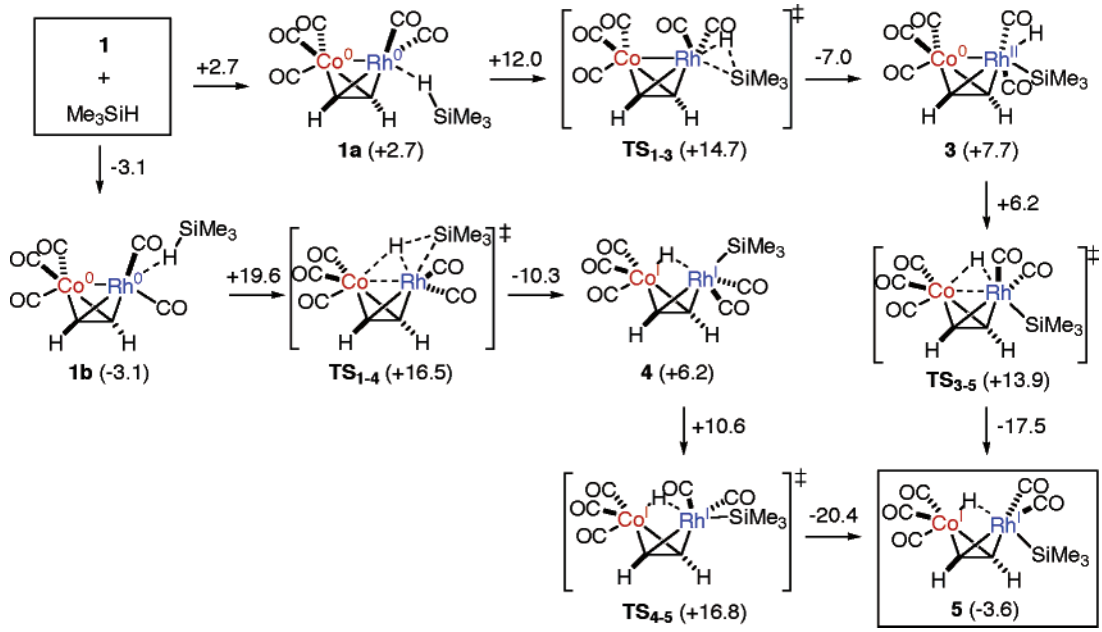

[a] Potential energies (kcal/mol, at the B3LYP/6311SDD//B3LYP/631LAN level) relative to [**1** + Me_3SiH] are shown in parentheses, and energy changes are shown together with arrows.

complex **1** and the oxidative addition product **5**, which are energetically comparable to each other (Scheme 5). Both pathways are stepwise and involve intermediary oxidative addition products (**3** and **4**). No pathway that leads directly to **5** could be located.

In path a, after formation of a precursor complex, **1a**,[28] Me_3SiH approaches the Rh center through the space between the two CO ligands on the Rh atom. In the transition state $\mathbf{TS}_{1-3}$ (Figure 3a), the Si−H bond is significantly elongated (1.995 Å, 33% increase from parent Me_3SiH (1.496 Å)), while the Rh−Si (2.533 Å) and Rh−H distances (1.606 Å) are close to that of the product **3** (Rh−Si: 2.472 Å, Rh−H: 1.587 Å). Thus, $\mathbf{TS}_{1-3}$ can be regarded as a very late transition state, and this process requires 14.7 kcal/mol activation energy (from **1** + Me_3SiH) and is endothermic by 7.7 kcal/mol. In the next step, the hydride on the Rh atom migrates to the Co atom via $\mathbf{TS}_{3-5}$ ($\Delta E^{\ddagger} = 6.2$ kcal/mol) to afford the hydride-bridged complex **5**, which is more stable than **3** by ca. 10 kcal/mol.

In path b, Me_3SiH undergoes oxidative addition through $\mathbf{TS}_{1-4}$, where the Si−H bond comes in across the Co−Rh bond. Through this TS, the Rh−Si bond formation, the Co−H(- -Rh) bond formation, and the Co−Rh bond cleavage take place in a concerted manner. $\mathbf{TS}_{1-4}$ is also a late transition state, as judged from the long Si−H distance (1.950 Å, 30% increase from Me_3SiH). The activation energy (+16.5 kcal/mol) is slightly higher than that of path a (14.7 kcal/mol). Rearrangement of **4** takes place with a moderate activation barrier ($\Delta E^{\ddagger} = 10.6$ kcal/mol) to give the complex **5** through a Berry pseudorotation-type TS ($\mathbf{TS}_{4-5}$).

(28) The energy of complex **1a** is slightly higher (2.7 kcal/mol) than that of [**1** + Me_3SiH]. This is due to the change of the orientation of two CO ligands on the Rh atom: While the CO ligands are coplanar with the Rh−Co-acetylene moiety in **1**, they are out of the plane in **1a**. Without the silane coordination, this orientation gives complex **1c**, which is less stable than **1** by 14.5 kcal/mol (at the B3LYP/631LAN level). Thus, **1a** is less stable than [**1** + Me_3SiH] but more stabilized compared with [**1c** + Me_3SiH].

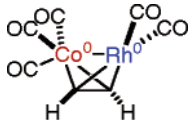

1c

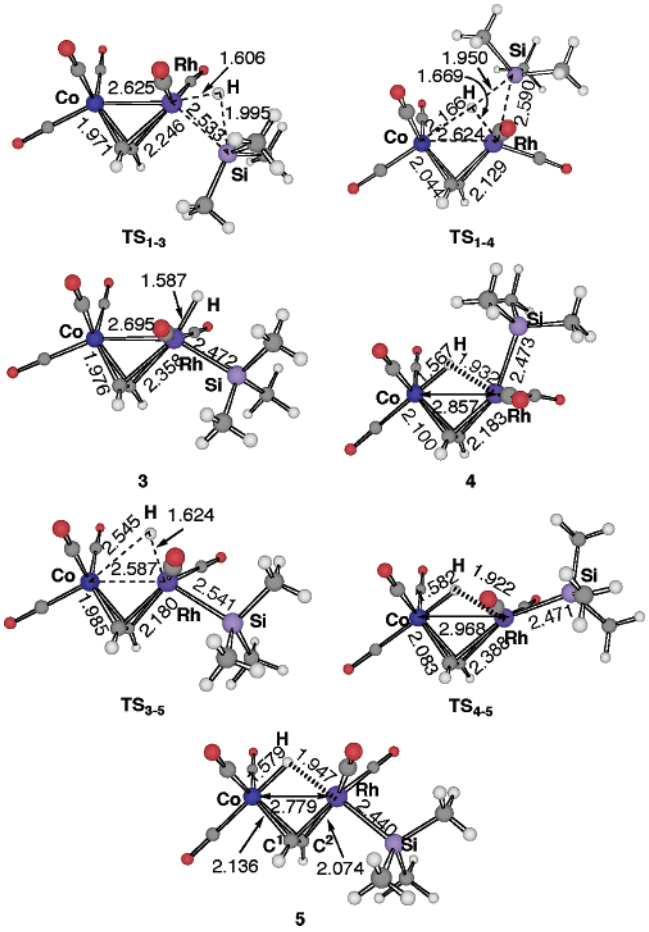

Figure 3. Structures of transition states and intermediates involved in the oxidative addition−isomerization processes (Scheme 5, at the B3LYP/631LAN level). Numbers refer to interatomic distances in Å.

The formal oxidation state of the metal atoms of **5** is of note. Since the silyl and hydride ligands are covalently bonded to the Rh and the Co atoms, respectively (Rh−H is a dative bond), both metal atoms are in the +1 oxidation state; both metals undergo one-electron oxidation throughout the conversion from **1** to **5**; that is, the Rh atom possesses d-electrons capable of back-donating to the acetylene. In fact, the bond lengths (Co−C^1: 2.136 Å, Rh−C^1: 2.074 Å), the bond angle ($\angle C^2-C^1-H$ = 141.2°), and the dihedral angles ($\angle Co-C^2-C^1-H$ = 119.2°, $\angle Rh-C^1-C^2-H$ = 152.6°) of **5** suggest that the Rh atom is dominant in the back-donation to the acetylene (Figure 3). Thus, if acetylene is considered to have formed a metallacycle, **5** must be regarded as a Co(I)-coordinated rhodio(III)cyclopropene. Note that the opposite situation was found in complex **1** (vide supra).

Acetylene Insertion. The Rh^I moiety of complex **5** takes a trigonal bipyramidal (TBP) structure, where the silyl and alkyne ligands are at the axial and equatorial positions, respectively. Such a coordination environment has been found in an olefin insertion precursor in a Rh-catalyzed hydroformylation reaction, that is, a TBP $HRh^I(C_2H_4)(CO)_2(PR_3)$ with an axial hydride and an equatorial ethylene.[29] Acetylene insertion into the Rh−Si bond takes place via a four-centered TS (**TS_{5-6}**, $\Delta E^{\ddagger}$ = 18.2 kcal/mol) to give the square planar, vinylrhodium intermediate **6** with large exothermicity (−11.7 kcal/mol) (Scheme 6 and Figure 4). The hydride bridge between the metals and the coordination of the Co atom to the C−C multiple bond are maintained throughout the process. The mechanism of this step dictates the Rh and the Si groups to be *cis* to each other and, hence, the final silylformylation product to be exclusively *Z*. The intermediate **6** may also prematurely decompose to give a *cis*-hydrosilylation side product. This has been observed experimentally (vide supra).[30,31]

Scheme 6. Acetylene Insertion into the Rh−Si Bond[a]

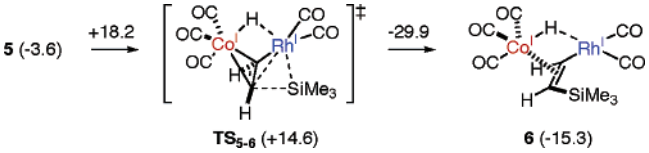

[a] Potential energies (kcal/mol, at the B3LYP/6311SDD//B3LYP/631LAN level) relative to [**1** + Me_3SiH] are shown in parentheses, and energy changes are shown together with arrows.

CO Insertion. The 16-electron complex **6** can accept one CO ligand, forms **7**, and gains stabilization of 9.2 kcal/mol. The complex **7** undergoes CO insertion via **TS_{7-8}** with a moderate activation energy (20.0 kcal/mol) to afford the acylrhodium intermediate **8** (Scheme 4, Figure 5).[32] On the other hand, direct CO insertion of complex **6** requires a higher activation energy (22.9 kcal/mol) to give a highly coordinatively unsaturated (14-electron) Rh complex. The step (**7** to **8**) is endothermic (+6.7 kcal/mol), but the reaction as a whole is irreversible because the subsequent steps (hydride migration−reductive elimination to the final product **10**) require much lower activation barriers than the reverse reaction (Figure 1, vide infra).

In the theoretical study on the Rh-catalyzed hydroformylation reaction, Morokuma et al. showed that CO insertion of a pentacoordinated Rh^I complex takes place through a TBP TS with an alkyl ligand in the equatorial plane and the carbonyl at the axial site (Scheme 7).[33b] On the other hand, the Rh center of **TS_{7-8}** takes an opposite geometry (vinyl at the axial site and CO in the equatorial plane) because the Rh−vinyl bond is firmly held through assistance by the Co−H moiety. The CO insertion of **7** is less endothermic than the reaction illustrated in Scheme 7 (ΔE = ca. +10 kcal/mol). This is probably due to extra stabilization of the Rh center by the semibridging CO ligand in the product **8** (Rh−C: 2.321 Å), which might compensate to some extent the energy loss due to the coordinative unsaturation upon going from **7** (16-e complex) to **8** (14-e complex).

Reductive Elimination. For the completion of the catalytic cycle, reductive elimination of the hydride and the acyl groups must take place from the complex **8**. Since the hydride and acyl groups are bound to different metals, the pathway of reductive elimination is an intriguing mechanistic subject.[5] There are a priori two mechanistic possibilities (Scheme 8), which are (a) direct and concerted reductive elimination from **8** and (b) sequential hydride shift from Co to Rh and reductive elimination at the Rh center. Since the first possibility is very intriguing, we extensively explored the potential surface; however, all

(29) (a) Koga, N.; Jin, S. Q.; Morokuma, K. *J. Am. Chem. Soc.* **1988**, *110*, 3417. (b) Matsubara, T.; Koga, N.; Ding, Y.; Musaev, D. G.; Morokuma, K. *Organometallics* **1997**, *16*, 1065−1078.

(30) The hydrosilylation reaction (in the absence of CO) with the same or related catalysts gives a *trans* adduct as a major product. A mechanism involving a zwitterionic carbene complex as a channel to the *trans* adduct has been proposed (ref 35). Although we examined the possibility for rotation of the C^1-C^2 bond of the vinylrhodium intermediates **6** and **7**, no stationary points have been located so far. It would be reasonable that the formation of the *trans* adduct would be prevented by the coordination of the C^1-C^2 double bond to the Co center.

(31) Ojima, I.; Clos, N.; Donovan, R. J.; Ingallina, P. *Organometallics* **1990**, *9*, 3127−3133.

(32) CO insertion from **6** was also examined and was energetically unfavorable.

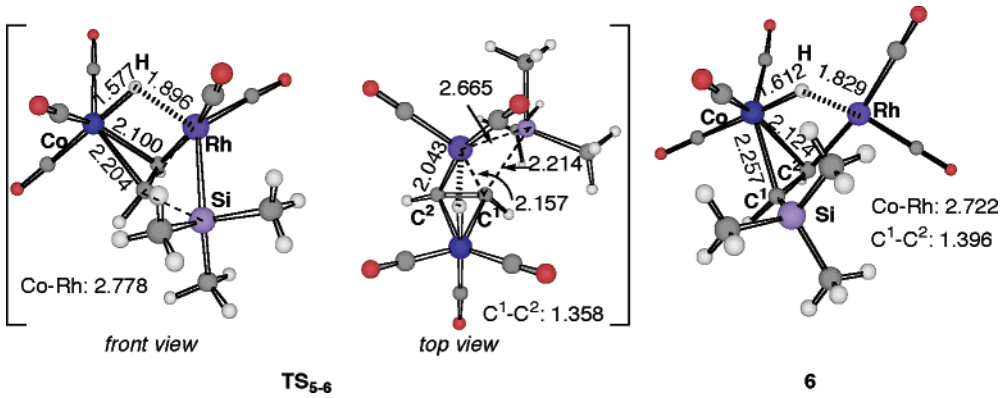

Figure 4. Structures of transition state and product of acetylene insertion (at the B3LYP/631LAN level). Numbers refer to interatomic distances in Å.

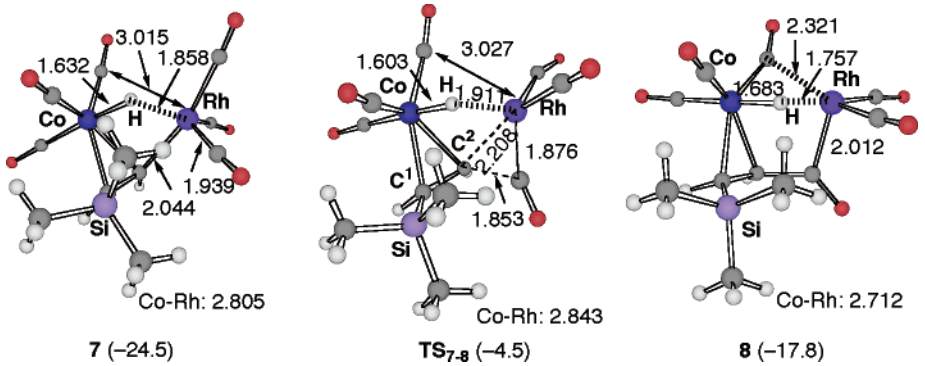

Figure 5. Structures of the stationary points along the CO insertion pathway (B3LYP/631LAN). Numbers in the structures and in the parentheses refer to interatomic distances and potential energies (B3LYP/6311SDD//B3LYP/631LAN), respectively.

Scheme 7. Pathways of CO Insertion of $Rh^{I}Et(CO)L_3$ (L = CO or PH_3)

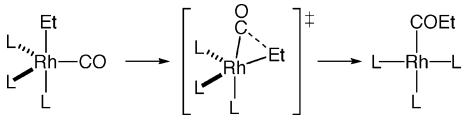

Scheme 8. Schematic Illustration of Possible Pathways of Reductive Elimination from the Co^{I}-Hydride/Acyl-Rh^{I} Complex

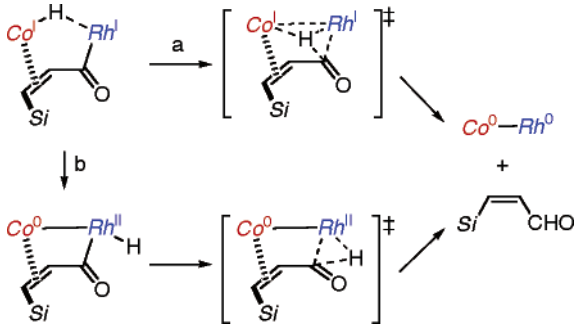

attempts invariably led to a single pathway along the second possibility. After all, this concerted/stepwise issue is experimentally irrelevant in the context of the overall catalytic cycle since the second pathway requires a very low barrier compared with the preceding steps (Figure 1).

The hydride shift occurs via $\mathbf{TS_{8-9}}$ with an activation energy of 2.3 kcal/mol to give the acylrhodium hydride complex **9** (Scheme 9, Figure 6). The intermediate **9** is slightly (1.9 kcal/mol) less stable than **8**. Upon hydride migration, the hydride becomes no longer bridged between Co and Rh (Co−H: 1.683 to 2.648 Å, Rh−H: 1.757 to 1.593 Å), and the semibridging

Scheme 9. Stepwise Reductive Elimination Pathway[a]

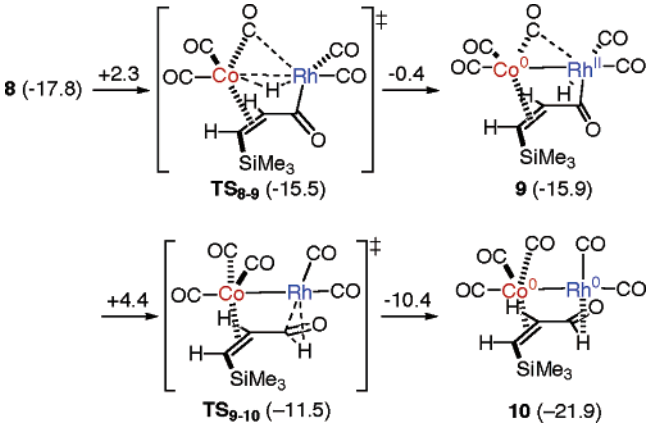

[a] Potential energies (kcal/mol, at the B3LYP/6311SDD//B3LYP/631LAN level) relative to [**1** + Me_3SiH] are shown in parentheses, and energy changes are shown together with arrows.

carbonyl ligand dissociates from the Rh center (2.321 to 2.500 Å). The intermediate **9** readily undergoes reductive elimination via a three-centered TS ($\mathbf{TS_{9-10}}$, $\Delta E^{\ddagger}$ = 4.4 kcal/mol) to give the final product **10**. During the reductive elimination, the Co−Rh bond is being regenerated (2.709 (**9**) → 2.641 ($\mathbf{TS_{9-10}}$) → 2.603 Å (**10**)). Replacement of the product, 3-trimethylsilylpropenal, by an acetylene molecule liberates the product and regenerates the initial butterfly complex **1**. The ligand exchange is a thermodynamically very favorable process; [**1** + 3-trimethylsilylpropenal] is more stable than [**10** + C_2H_2] by 23.3 kcal/mol.

Figure 7 summarizes the changes of interatomic distances along the catalytic cycle. From the changes of the Co−Rh, Rh−H, and Co−H distances, one can understand the correlation of

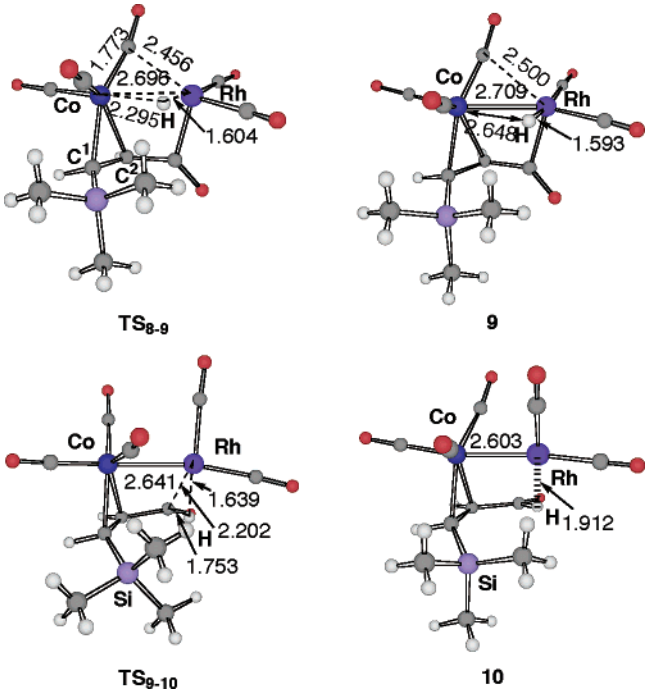

Figure 6. Structures of stationary points along reductive elimination. Numbers refer to interatomic distances in Å.

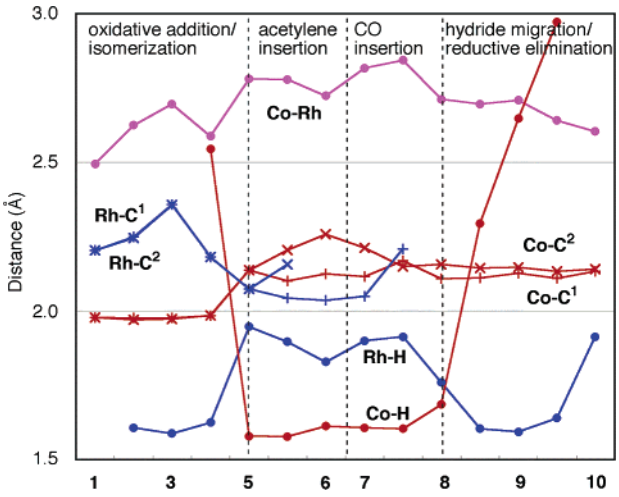

Figure 7. Changes of interatomic distances (Å) along the catalytic cycle.

the events including the Co−Rh bond cleavage/formation and the hydride transfer from Rh to Co (and vice versa). The Rh−C^1 and Rh−C^2 distances become shorter than the Co−C distances upon formation of the complex **5**. As discussed above, this reflects strong back-donation from Rh to the acetylene in **5**. The C^1−C^2 unsaturated bond coordinates to the Co atom throughout the reaction pathway. The Co atom is equally bonded to the C^1 and C^2 atoms during the catalytic cycle except for the period between the acetylene insertion and CO insertion steps (Co−C^2 is shorter than Co−C^1). This is presumably because the α-carbon atom (C^2) of the vinylrhodium intermediate is more Lewis basic than the *β*-carbon atom (C^1).

Figure 8 summarizes the natural population analysis along the catalytic cycle. One can easily follow the charges on the acetylene moiety and the Me_3Si group. The acetylene moiety is negatively charged from the beginning due to back-donation and becomes much more negative at the acetylene insertion stage (i.e., Rh−C bond formation). The Me_3Si group first becomes less positive upon the oxidative addition (i.e., Rh−Si bond

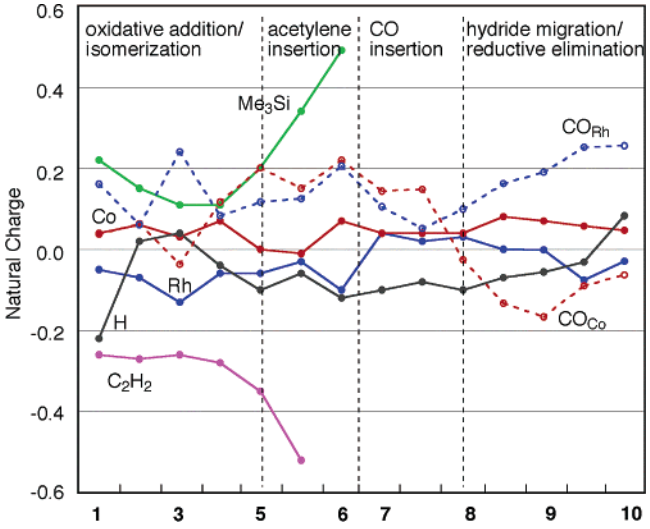

Figure 8. Natural population analysis of Co, Rh, acetylene, Me_3-Si, H (hydride), and CO along the catalytic cycle. CO_{Co} and CO_{Rh} indicate sums of charges of CO ligands bound to the Co and the Rh atoms, respectively.

formation) and then becomes more positive at the acetylene insertion stage (i.e., C−Si bond formation). The correlation between the reaction pathway and the natural charges of the two metals is less obvious. The charges remain within a very narrow range (−0.01 to 0.08 for Co, −0.13 to 0.04 for Rh) while the reaction involves formal oxidative addition/reductive elimination steps. The CO ligands act as a buffer to moderate the charge change of the metal atoms by donating or accepting electrons to/from the metal centers, as judged from rather drastic charge change of the CO ligands.

Regio- and Stereoselectivity of Silylformylation Reaction. Since the carbon−silicon bond formation is the regioselectivity-determining step of the silylformylation reaction, we examined insertion of propyne into a Rh−Si bond employing a model complex, **5′** (Scheme 10). In agreement with the experimental selectivity (see Introduction), the silicon delivery to the terminal carbon atom via $\mathbf{TS_{5'-6'}}$ ($\Delta E^{\ddagger}$ = 17.3 kcal/mol) is much more favorable than to the methyl-substituted carbon atom via $\mathbf{TS_{5'-6''}}$ ($\Delta E^{\ddagger}$ = 28.8 kcal/mol). $\mathbf{TS_{5'-6''}}$ suffers from steric repulsion between the Me_3Si group and the methyl substituent. The activation energy of 17.3 kcal/mol for $\mathbf{TS_{5'-6'}}$ is essentially the same as that of 18.2 kcal/mol for $\mathbf{TS_{5-6}}$ determined for unsubstituted acetylene (Figure 4).

In summary, we have explored the bimetallic reaction pathway of the Co/Rh mixed-metal-catalyzed silylformylation of alkyne. The overall mechanism can be regarded as an intriguing hybrid of the two proposed mechanisms (Scheme 1) based on the hydrosilylation and the hydroformylation reactions (Scheme 11): oxidative addition of Si−H to Rh^0 (step i, see also Scheme 1a), Rh-to-Co hydride migration and Co−Rh bond cleavage (step i′), alkyne insertion into the Rh^I−Si bond (step ii, see also Scheme 1b), carbonyl insertion into the Rh^I−C bond (step iii, see also Scheme 1b), Co-to-Rh hydride migration and Co−Rh bond formation (step iii′), and reductive elimination of acylrhodium(II) hydride (step iv, see also Scheme 1a). The dominant role of the Rh atom agrees with our experimental knowledge that Rh, but not Co, has generally been useful for this class of reaction.[14−18] The most mechanistically intriguing aspect is the dynamic behavior of the Co/Rh bimetallic structure throughout the catalytic cycle. The metal−metal bond formation and the hydride bridging serve as complementary ways for the catalyst to maintain its bimetallic structure. While all of the

Scheme 10. Insertion of Propyne into the Rh−Si Bond of 5′

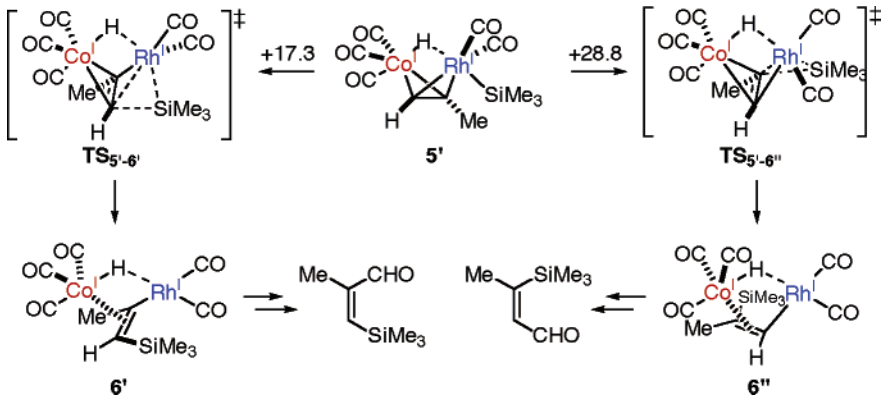

Scheme 11. Schematic Catalytic Cycle of Co/Rh Bimetallic Silylformylation

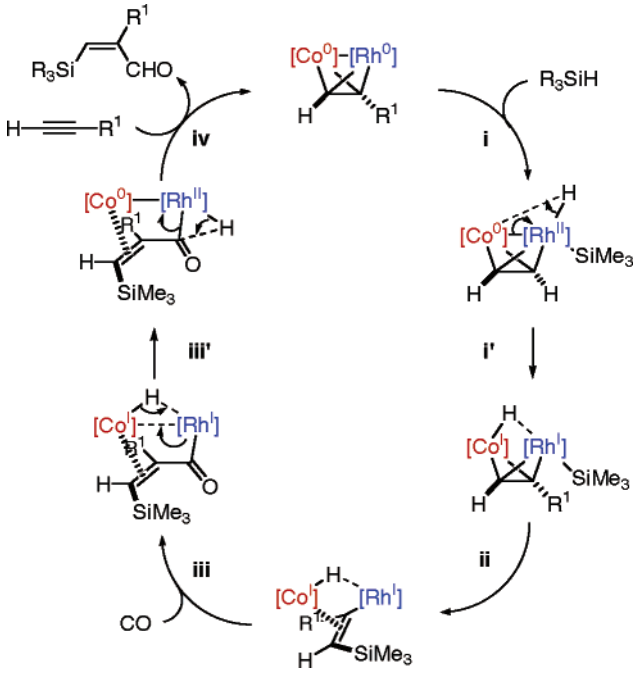

bond-forming events take place at the Rh center, the Co center also plays important roles to fix the substrate, keep the hydride, and deliver it back to Rh prior to reductive elimination.

The bimetallic synergism delineated here reminds us of the mechanisms of other bimetallic catalyses: The reversibility of metal−metal bond formation (reinforcement) and cleavage (weakening) is commonly found in catalysis of multinuclear transition metal (TM) complexes, as previously demonstrated in the PK reaction,[3a] the dirhodium-catalyzed C−H bond insertion of diazo compounds,[3b] and the diruthenium-catalyzed propargylic substitution.[3c] In the latter two cases, bridging spectator ligands (carboxylate for Rh−Rh and thiolate for Ru−Ru) maintain the bimetallic structure while the metal−metal bond is cleaved. On the other hand, the hydride ligand, the participant of the catalysis, plays this role in the present system. While such systems of dinuclear TM complexes effectively promote the unique synthetic transformations, the synergy of the TM nucleophilicity and the main group metal (MM) Lewis acidity gives rise to the driving force of a number of TM/MM catalyses.[33,34]

Acknowledgment. This collaborative work was initiated by the NSF-JSPS International Collaborative Research program (NSF INT-9726789 to I.O., 1998−2001). We thank the Ministry of Education, Culture, Sports, Science and Technology, the 21st Century COE Program in Fundamental Chemistry, and computational time from Research Center for Computational Science, Okazaki National Research Institute and Intelligent Modeling Laboratory, The University of Tokyo.

Supporting Information Available: Energies and Cartesian coordinates of stationary points and details of oxidative addition of Me_3SiH. This material is available free of charge via the Internet at http://pubs.acs.org.

OM060478X

(33) Nakamura, E.; Mori, S. *Angew. Chem., Int. Ed.* **2000**, *39*, 3750−3771, and references therein.

(34) (a) Yoshikai, N.; Nakamura, E. *J. Am. Chem. Soc.* **2004**, *126*, 12264−12265. (b) Yamanaka, M.; Nakamura, E. *J. Am. Chem. Soc.* **2005**, *127*, 4697−4706. (c) Yoshikai, N.; Mashima, H.; Nakamura, E. *J. Am. Chem. Soc.* **2005**, *127*, 17978−17979.